

## Syntheses of the Eastern Halves of Ritterazines B, F, G, and H, Leading to Reassignment of the 5,5-Spiroketal Stereochemistry of Ritterazines B and F

Scott T. Phillips and Matthew D. Shair\*

Contribution from the Department of Chemistry & Chemical Biology, Harvard University, Cambridge, Massachusetts 02138

Received January 29, 2007; E-mail: shair@chemistry.harvard.edu

**Abstract:** The ritterazine class of natural products comprises 26 compounds—all of which are spiroketal-containing steroidal heterodimers—that inhibit the proliferation of cultured human cancer cell lines with IC<sub>50</sub> values in the low nanomolar range. Little is known about their chemistry, cellular target(s), or mechanism(s) of growth inhibition, due primarily to the small amount of material available from natural sources. In this paper we report syntheses of the eastern halves of ritterazines B, F, G, and H and address the energetic and mechanistic aspects of spiroketal equilibration for each. These studies have led to reassignment of the 5,5-spiroketal stereochemistry of ritterazines B and F, and they have enabled us to propose a quantitative description of the natural distribution of these ritterazine compounds.

### Introduction

Ritterazine B, a marine natural product reported by Fusetani et al. in 1995,<sup>1</sup> is the most potent inhibitor of cultured human cancer cell lines of the 26 known ritterazine compounds.<sup>1–4</sup> Its average GI<sub>50</sub> value is 3.2 nM in the National Cancer Institute's 60-cell-line screen,<sup>5</sup> and in fact, ritterazine B is among the most potent growth inhibitors ever tested by the National Cancer Institute (NCI).<sup>5</sup> However, the effects of ritterazine B on cells and its potential as an anticancer treatment have not been studied in depth due to lack of material.<sup>6</sup> The structurally related natural product cephalostatin 1<sup>7,8</sup> has a pattern of cytotoxicity similar to that of ritterazine B in 10 of the NCI cell lines (NCI-10) (with a Pearson correlation coefficient of 0.93),<sup>6,9</sup> suggesting that both compounds may have similar or identical cellular target(s) and mechanism(s). Since early studies have shown interesting effects of cephalostatin 1 on cells,<sup>10</sup> the same may

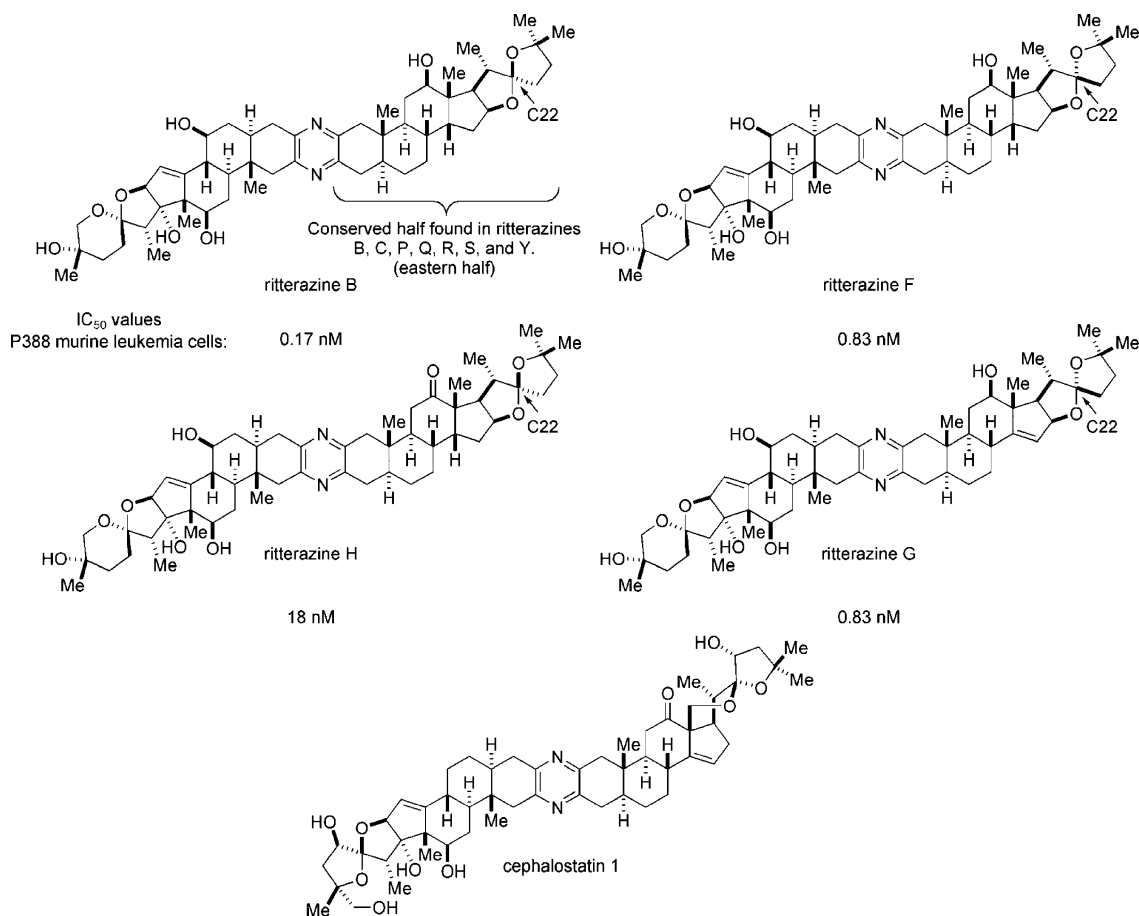
be true of ritterazine B. The lack of correlation between the cytotoxicity patterns of ritterazine B or cephalostatin 1 with molecules of known mechanism suggests that these natural products also may have unique mechanisms.<sup>5,7,9–13</sup>

We have become interested in answering the following questions surrounding the cephalostatins and the ritterazines: (1) Do these compounds show some selective cytotoxic or cytostatic effects for tumor cells versus nontransformed cells, and does this activity translate to in vivo effects? (2) What are the cellular target(s) and mechanism(s) of these molecules, and are they related? (3) Might these compounds reveal new anticancer cellular targets? (4) Which portions of these large heterodimers are responsible for their biological activity? (5) Why are certain ritterazine family members found in nature, while other expected derivatives are not? Several of these compelling questions could be answered if sufficient quantities of the natural products were available (which they are not),<sup>14,15</sup> but others only can be addressed by preparing derivatives by synthesis. Therefore, efficient syntheses capable of accessing hundreds of milligrams of these natural products and their derivatives are needed.

We have initiated a program to study the chemistry and biology of the most active ritterazines (shown in Chart 1) and cephalostatin 1. With respect to the ritterazines, the western

- (1) Fukuzawa, S.; Matsunaga, S.; Fusetani, N. *J. Org. Chem.* **1995**, *60*, 608–614.
- (2) Fukuzawa, S.; Matsunaga, S.; Fusetani, N. *J. Org. Chem.* **1994**, *59*, 6164–6166.
- (3) Fukuzawa, S.; Matsunaga, S.; Fusetani, N. *Tetrahedron* **1995**, *51*, 6707–6716.
- (4) Fukuzawa, S.; Matsunaga, S.; Fusetani, N. *J. Org. Chem.* **1997**, *62*, 4484–4491.
- (5) Flessner, T.; Jautelat, R.; Scholz, U.; Winterfeldt, E. *Fortschritte der Chemie Organischer Naturstoffe*; Springer-Verlag: New York, 2004.
- (6) Komiya, T.; Fusetani, N.; Matsunaga, S.; Kubo, A.; Kaye, F. J.; Kelley, M. J.; Tamura, K.; Yoshida, M.; Fukuoka, M.; Nakagawa, K. *Cancer Chemother. Pharmacol.* **2003**, *51*, 202–208.
- (7) Pettit, G. R.; Inoue, M.; Kamano, Y.; Herald, D. L.; Arm, C.; Dufresne, C.; Christie, N. D.; Schmidt, J. M.; Doubek, D. L.; Krupa, T. S. *J. Am. Chem. Soc.* **1988**, *110*, 2006–2007.
- (8) Müller, I. M.; Dirsch, V. M.; Rudy, A.; López-Antón, N.; Pettit, G. R.; Vollmar, A. M. *Mol. Pharm.* **2005**, *67*, 1684–1689.
- (9) Paull, K. D.; Shoemaker, R. H.; Hodes, L.; Monks, A.; Scudiero, D. A.; Rubinstein, L.; Plowman, J.; Boyd, M. R. *J. Natl. Cancer Inst.* **1989**, *81*, 1088–1092.
- (10) López-Antón, N.; Rudy, A.; Barth, N.; Schmitz, L. M.; Pettit, G. R.; Schulze-Osthoff, K.; Dirsch, V. M.; Vollmar, A. M. *J. Biol. Chem.* **2006**, *281*, 33078–33086.

- (11) Rabow, A. A.; Shoemaker, R. H.; Sausville, E. A.; Covell, D. G. *J. Med. Chem.* **2002**, *45*, 818–840.
- (12) Boyd, M. R. *The NCI In Vitro Anticancer Drug Discovery Screen*; Humana Press Inc.: Totowa, NJ, 1985–1995.
- (13) Boyd, M. R.; Paull, K. D. *Drug Dev. Res.* **1995**, *34*, 91–109.
- (14) A 13.4 mg sample of ritterazine B was isolated from 5.5 kg of *Ritterella tokioka*, and 139 mg of cephalostatin 1 was obtained from 166 kg of *Cephalodiscus gilchristi* (wet mass).
- (15) LaCour, T. G.; Guo, C.; Ma, S.; Jeong, J. U.; Boyd, M. R.; Matsunaga, S.; Fusetani, N.; Fuchs, P. L. *Bioorg. Med. Chem. Lett.* **1999**, *9*, 2587–2592.

**Chart 1.** Structures and Biological Activities for Ritterazines B, F, G, and H and Cephalostatin 1

halves are conserved, while minor structural changes in the eastern halves cause substantial variations in growth inhibitory activity. Since the activity of these compounds is dependent on the eastern halves, we focused on preparing and studying these portions as an important step toward studying the entire class of compounds. In this paper we report syntheses of the eastern halves of ritterazines B, F, G, and H, as well as the spiroketal epimers of ritterazines G and H. Structural analyses of these halves have led us to reassign the ritterazine B and F spiroketal stereochemistry (C22) (and therefore those of six other ritterazines). Also, kinetics studies have been used to explain the natural distribution of these ritterazine spiroketals and to predict other, as of yet, undiscovered ritterazine natural products.

## Results and Discussion

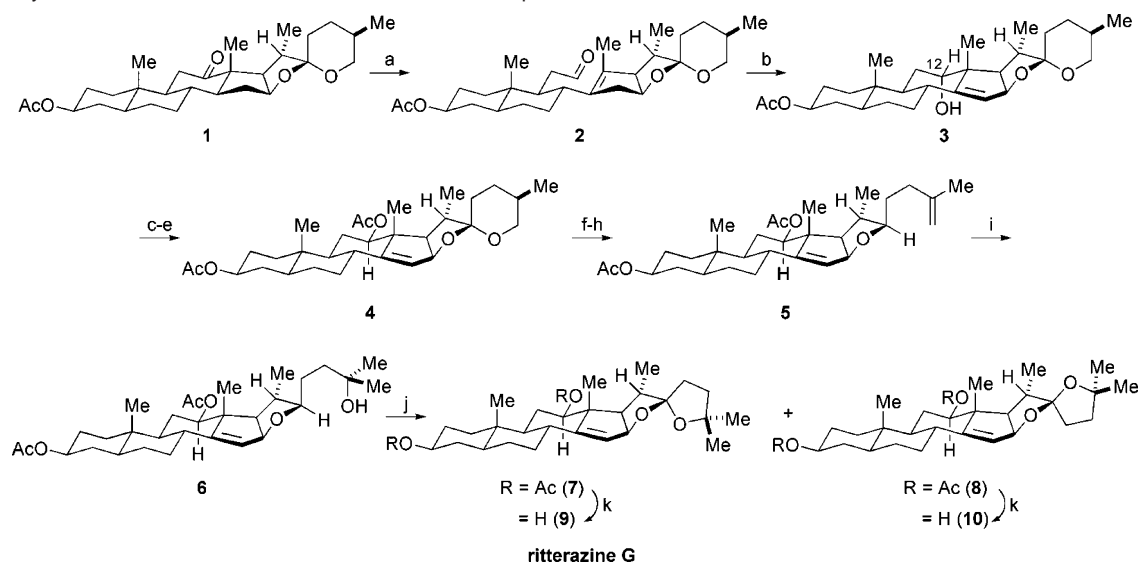
**Synthesis of the Ritterazine G Eastern Half.** To study the eastern halves of ritterazines B, F, G, and H, we required an efficient and scalable synthesis of the ritterazine G eastern half: from it, we planned to access the other eastern halves in a few additional steps. A great deal of chemistry for building these bis-steroidal natural products has been developed by Fuchs and co-workers, particularly with respect to the cephalostatins.<sup>16–25</sup>

Less progress has been made on the ritterazines, though Fuchs and co-workers have made important contributions here as well by developing routes to ritterazines K<sup>21</sup> and M,<sup>26</sup> by reassigning ritterazine M,<sup>27</sup> and by synthesizing the eastern halves of ritterazines G<sup>24</sup> and I.<sup>28</sup> Chemistry for related compounds also has been developed by Winterfeldt,<sup>29–38</sup> Heathcock,<sup>39,40</sup> Tietze,<sup>41,42</sup> Suárez,<sup>43,44</sup> and others.<sup>16,17</sup>

Fuchs has shown that carrying the ritterazine G eastern half through many steps causes epimerization of the spiroketal,

- (16) Ganesan, A. *Angew. Chem. Int. Ed. Engl.* **1996**, *35*, 611–615.
- (17) Grysckiewicz-Wojtkielewicz, A.; Jastrzebska, I.; Morzycki, J. W.; Romanowska, D. B. *Curr. Org. Chem.* **2003**, *7*, 1257–1277.
- (18) Guo, C.; Bhandaru, S.; Fuchs, P. L. *J. Am. Chem. Soc.* **1996**, *118*, 10672–10673.
- (19) Lee, J. S.; Fuchs, P. L. *Org. Lett.* **2003**, *5*, 2247–2250.
- (20) Lee, J. S.; Fuchs, P. L. *J. Am. Chem. Soc.* **2005**, *127*, 13122–13123.
- (21) Jeong, J. U.; Guo, C.; Fuchs, P. L. *J. Am. Chem. Soc.* **1999**, *121*, 2071–2084 and references therein.

- (22) Jeong, J. U.; Sutton, S. C.; Kim, S.; Fuchs, P. L. *J. Am. Chem. Soc.* **1995**, *117*, 10157–10158.
- (23) Kim, S.; Sutton, S. C.; Guo, C.; LaCour, T. G.; Fuchs, P. L. *J. Am. Chem. Soc.* **1999**, *121*, 2056–2070 and references therein.
- (24) LaCour, T. G.; Guo, C.; Bhandaru, S.; Boyd, M. R.; Fuchs, P. L. *J. Am. Chem. Soc.* **1998**, *120*, 692–707 and references therein.
- (25) Li, W.; LaCour, T. G.; Fuchs, P. L. *J. Am. Chem. Soc.* **2002**, *124*, 4548–4549.
- (26) Lee, S.; Fuchs, P. L. *Org. Lett.* **2002**, *4*, 317–318.
- (27) Lee, S.; LaCour, T. G.; Lantrip, D.; Fuchs, P. L. *Org. Lett.* **2002**, *4*, 313–316.
- (28) LaCour, T. G.; Fuchs, P. L. *Tetrahedron Lett.* **1999**, *40*, 4655–4658.
- (29) Bäsler, S.; Brunck, A.; Jautelat, R.; Winterfeldt, E. *Helv. Chim. Acta* **2000**, *83*, 1854–1880.
- (30) Flessner, T.; Ludwig, V.; Siebeneicher, H.; Winterfeldt, E. *Synthesis* **2002**, 1373–1378.
- (31) Haak, E.; Winterfeldt, E. *Synlett* **2004**, 1414–1418.
- (32) Jautelat, R.; Müller-Fahrmow, A.; Winterfeldt, E. *Chem.—Eur. J.* **1999**, *5*, 1226–1233.
- (33) Jautelat, R.; Winterfeldt, E.; Müller-Fahrmow, A. *J. Prakt. Chem./Chem.-Ztg.* **1996**, *338*, 695–701.
- (34) Drögemüller, M.; Flessner, T.; Jautelat, R.; Scholz, U.; Winterfeldt, E. *Eur. J. Org. Chem.* **1998**, 2811–2831.
- (35) Nawasreh, M.; Winterfeldt, E. *Curr. Org. Chem.* **2003**, *7*, 649–658.
- (36) Scholz, U.; Winterfeldt, E. *Nat. Prod. Rep.* **2000**, *17*, 349–366.
- (37) Winterfeldt, E. *Pure Appl. Chem.* **1999**, *71*, 1095–1099.
- (38) Yunus, U.; Iqbal, R.; Winterfeldt, E. *J. Heterocycl. Chem.* **2005**, *42*, 1079–1084.

**Scheme 1.** Synthesis of the Ritterazine G Eastern Half and Its Spiroketal Diastereomer<sup>a</sup>

<sup>a</sup> Reagents and conditions: (a) *hν*, dioxane; (b)  $\text{BF}_3 \cdot \text{OEt}_2$ , PhMe, 83% (two steps); (c) Jones oxidation; (d)  $\text{NaBH}_4$ ,  $-78^\circ\text{C}$ ; (e)  $\text{Ac}_2\text{O}$ , DMAP, 91% (three steps); (f)  $\text{NaCNBH}_3$ , AcOH, 93%; (g) *o*- $\text{NO}_2\text{PhSeCN}$ ,  $\text{PBu}_3$ ; (h)  $\text{H}_2\text{O}_2$ ,  $0^\circ\text{C}$ , 67% (two steps); (i)  $\text{Hg}(\text{OAc})_2$ , THF/ $\text{H}_2\text{O}$ ;  $\text{NaBH}_4$ , 88%; (j)  $\text{PhI}(\text{OAc})_2$ , 97% (7:8 = 2.7:1); (k)  $\text{K}_2\text{CO}_3$ , MeOH, 100%.

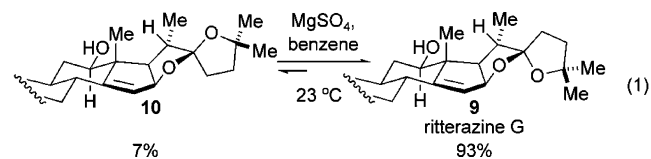
necessitating chromatographic separations. We decided to simplify the experimental difficulties in handling this spiroketal by performing a late-stage spiroketalization under conditions that were nonequilibrating, but that would allow us to prepare the two spiroketal epimers for each ritterazine half (meaning we needed routes for the preparation of ritterazines G and H and their spiroketal epimers and of ritterazines B and F). The reaction we chose to form the spiroketal was a Su rez oxidative spiroketalization (see Scheme 1).<sup>44</sup>

Our synthesis of the ritterazine G eastern half (Scheme 1) was accomplished in 40% yield over 10 steps from hecogenin acetate (**1**), a convenient and commercially available steroid building block. The first step, based on the work of Winterfeldt, is a Norrish type I photolytic cleavage of the C12–C13 bond, affording aldehyde **2**.<sup>34</sup>  $\text{BF}_3 \cdot \text{OEt}_2$ -catalyzed ene reaction on the unpurified aldehyde (compound **2**) proceeds to form a six-membered ring with the C12 secondary carbinol in the  $\alpha$ -configuration (compound **3**).<sup>34</sup> Ritterazine G has a  $\beta$ -configured secondary carbinol at this position, so an efficient sequence of oxidation and reduction steps is used to invert the alcohol.<sup>24</sup> Reductive opening<sup>29</sup> of spiroketal **4** affords a primary alcohol that is then converted to terminal olefin **5** using the selenation/oxidation protocol developed by Grieco.<sup>45</sup> Initially, we encountered variable yields (30–87%) when the selenation step was performed in THF. The variation appeared inversely dependent on the purity of the starting material (higher yields were obtained using the unpurified alcohol), which suggested the possibility that residual  $\text{NaHCO}_3$  from the previous workup had a beneficial effect on the Grieco

reaction. Reproducible, albeit somewhat lower, yields are obtained using purified alcohol and by changing the solvent to pyridine.<sup>45</sup>

Oxymercuration–demercuration of alkene **5** provides tertiary carbinol **6** in 88% yield, along with 12% recovered starting material. The demercuration step in this reaction is known to be accelerated by hydroxide,<sup>46</sup> but in our case, the presence of hydroxide significantly increased the amount of starting material recovered, even though the mercuration step was nearly quantitative. However, when sodium borohydride (without sodium hydroxide) is added directly to the reaction mixture, the demercuration step proceeds with a minimal amount of elimination.<sup>46</sup>

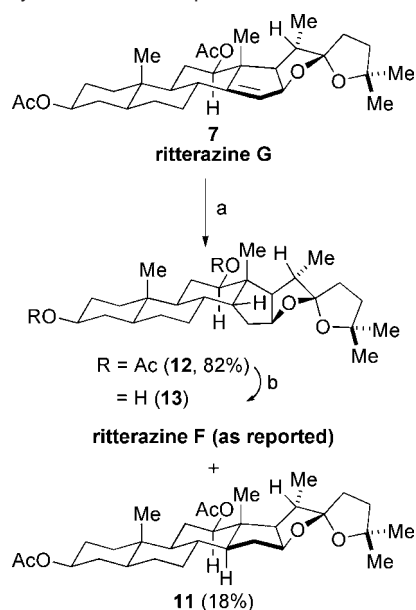
In the last step of our synthesis, a Su rez iodine(III) oxidation<sup>44</sup> is used to form a mixture of two epimeric 5,5-spiroketal in nearly quantitative yield, where the ritterazine G diastereomer (**7**) is the favored product. The two diastereomers can be separated by silica gel chromatography, providing access to both spiroketals for further studies. Alternatively, the crude mixture of spiroketals can be equilibrated over  $\text{MgSO}_4$  during workup to form the ritterazine G diastereomer almost exclusively (see eq 1).



**Syntheses of the Reported Ritterazine B and Ritterazine F Eastern Halves.** The reported ritterazine F eastern half was prepared in one step from the ritterazine G eastern half (**7**) using a Pt/C-catalyzed hydrogenation (Scheme 2). At the outset we expected hydrogenation to occur from the less hindered  $\alpha$ -face of the olefin,<sup>47</sup> but in this case, the allylic ether seems to direct

- (39) Heathcock, C. H.; Smith, S. C. *J. Org. Chem.* **1994**, *59*, 6828–6839.  
 (40) Heathcock, C. H.; Smith, S. C. *J. Org. Chem.* **1995**, *60*, 6641–6641.  
 (41) Tietze, L. F.; Krahnert, W. F. *Synlett* **2001**, 560–562.  
 (42) Tietze, L. F.; Krahnert, W. R. *Chem.–Eur. J.* **2002**, *8*, 2116–2125.  
 (43) Betancor, C.; Freire, R.; P rez-Mart n, I.; Prang , T.; Su rez, E. *Org. Lett.* **2002**, *4*, 1295–1297.  
 (44) Betancor, C.; Freire, R.; P rez-Mart n, I.; Prang , T.; Su rez, E. *Tetrahedron* **2005**, *61*, 2803–2814.  
 (45) Grieco, P. A.; Gilman, S.; Nishizawa, M. *J. Org. Chem.* **1976**, *41*, 1485–1486.

- (46) Brown, H. C.; Geoghegan, P. J., Jr. *J. Org. Chem.* **1970**, *35*, 1844–1850.  
 (47) Abad, A.; Agullo, C.; Arno, M.; Domingo, L. R.; Zaragoza, R. J. *J. Org. Chem.* **1990**, *55*, 2369–2373.

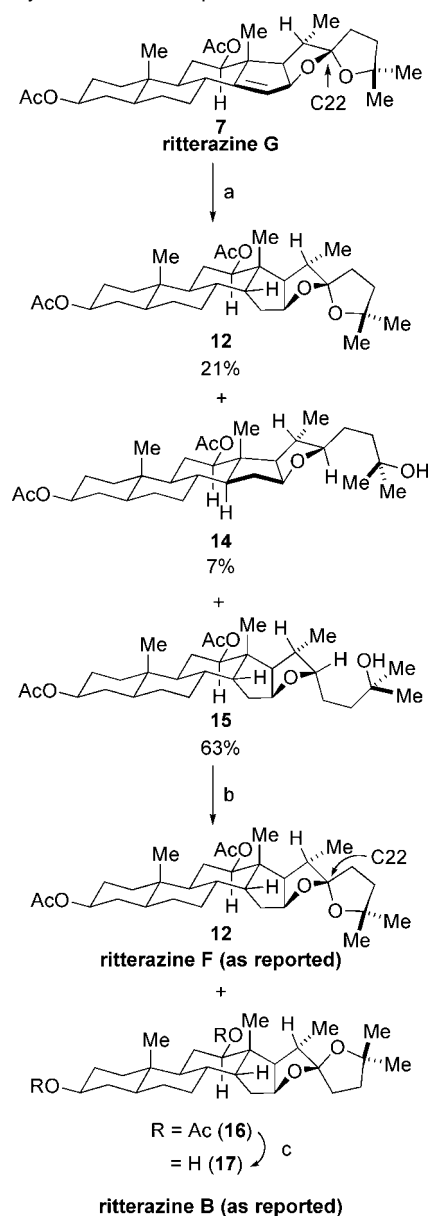
**Scheme 2.** Synthesis of the Reported Ritterazine F Eastern Half<sup>a</sup>

<sup>a</sup> Reagents and conditions: (a) Pt/C, H<sub>2</sub>, EtOH; (b) K<sub>2</sub>CO<sub>3</sub>, MeOH, 100%.

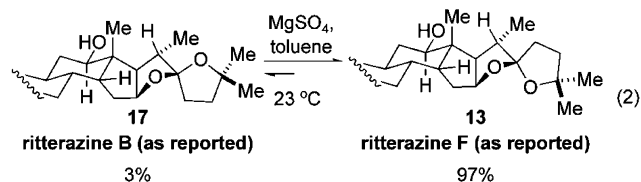
the heterogeneous catalyst to the hindered  $\beta$ -face,<sup>48</sup> providing ritterazine F in 82% yield. This procedure represents a particularly effective route to spiroketal-substituted *cis*-hydrindanes, which normally require several steps for their preparation from the corresponding *trans*-hydrindane steroidal precursors.<sup>49</sup> This hydrogenation also is striking in that other reagents (Pd(OH)<sub>2</sub>/C, PtO<sub>2</sub> in EtOH, Crabtree's catalyst, Wilkinson's catalyst, hydroboration/protonolysis, and 5% rhodium on alumina) were ineffective and only provided starting material.

A similar hydrogenation of the C22 epimer of ritterazine G (compound **8**, Scheme 1) provided little of the desired ritterazine B eastern half. Whereas the conversion of ritterazine G to ritterazine F involved the hydrogenation of one thermodynamic spiroketal to form another, the spiroketal in the non thermodynamically favored configuration (due to one anomeric effect) (compound **8**) presented unexpected problems. In this case, compound **8** equilibrated in ethanol at a rate competitive with that for hydrogenation, leading to a mixture of products favoring ritterazine G, ritterazine F, and a *trans*-hydrindane impurity.<sup>50</sup> Alternatively, we accessed the structure reported to be the eastern half of ritterazine B through a more circuitous path (Scheme 3). Hydrogenation of the eastern half of ritterazine G (7), rather than its non thermodynamically favored C22 epimer, in acetic acid (instead of ethanol) delivers the *cis*-hydrindane and reduces the spiroketal, affording **15** in 63% yield. Suárez spiroketalization<sup>44</sup> of **15** then forms a separable mixture of the eastern halves of ritterazines B (**16**) and F (**12**) in quantitative yield, where the eastern half of ritterazine B (**16**) is the less abundant C22 spiroketal epimer.

Like the eastern halves of ritterazine G and its diastereomer, the spiroketals of the eastern halves of ritterazines B and F interconvert under slightly Lewis acidic conditions, with the equilibrium favoring ritterazine F (see eq 2). The ritterazine F

**Scheme 3.** Synthesis of the Reported Ritterazine B Eastern Half<sup>a</sup>

<sup>a</sup> Reagents and conditions: (a) Pt/C, H<sub>2</sub>, AcOH; (b) PhI(OAc)<sub>2</sub>, I<sub>2</sub>, 100% (**12**:**16** = 3:1); (c) K<sub>2</sub>CO<sub>3</sub>, MeOH, 100%.

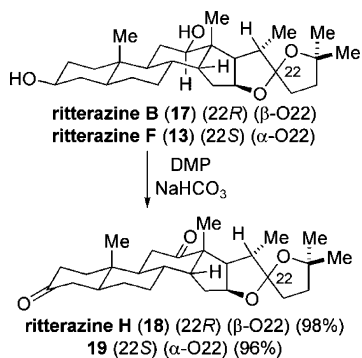


diastereomer can be obtained almost exclusively from the Suárez reaction if the workup includes MgSO<sub>4</sub> instead of Na<sub>2</sub>SO<sub>4</sub> as the drying reagent, though such an equilibration is unnecessary since ritterazine F can be accessed more efficiently as outlined in Scheme 2. Overall, the ritterazine F eastern half can be prepared in 11 steps and 33% yield from hecogenin acetate. The ritterazine B eastern half is accessed less efficiently in 6% yield over 12 steps from hecogenin acetate; the major loss of material in this sequence occurs in the final Suárez reaction, where the more stable (*S*)-C22 spiroketal (**12**) predominates over the ritterazine B eastern half (Scheme 3).

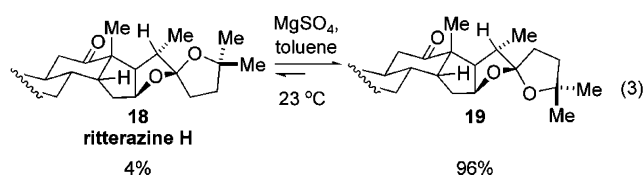
(48) Hoveyda, A. H.; Evans, D. A.; Fu, G. C. *Chem. Rev.* **1993**, *93*, 1307–1370.

(49) Jung, M. E.; Johnson, T. W. *Tetrahedron* **2001**, *57*, 1449–1481.

(50) Each product was synthesized through an independent route as shown in Schemes 1–3. Chemical shift data for all compounds are tabulated in the Supporting Information.

**Scheme 4.** Synthesis of the Ritterazine H Eastern Half and Its Spiroketal Epimer

**Synthesis of the Ritterazine H Eastern Half.** The eastern half of ritterazine H and its C22 spiroketal epimer were prepared by oxidation of ritterazines B and F, respectively (Scheme 4). Not surprisingly, under equilibrating conditions the spiroketal of the eastern half of ritterazine H is converted into the thermodynamically more stable C22 epimer (**19**) (see eq 3).

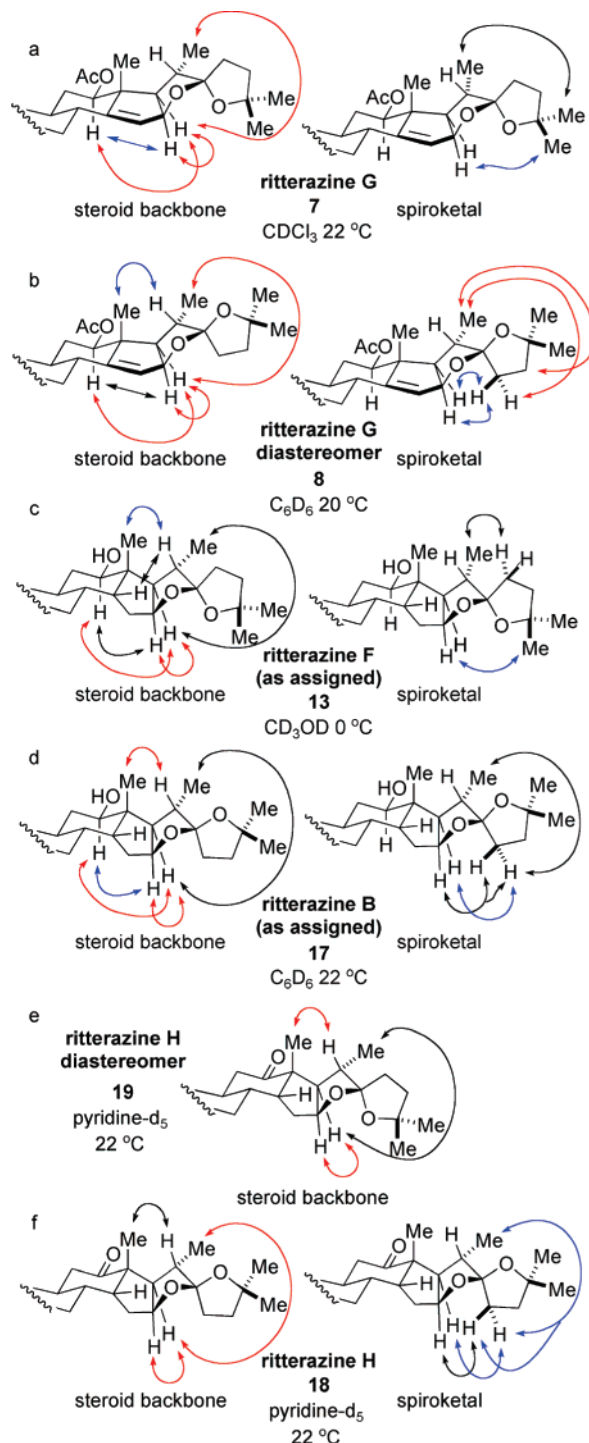


Compound **19** is stabilized by two anomeric effects, whereas compound **18** is only stabilized by one anomeric effect. The ease of this equilibration indicates the importance of avoiding both Brønsted and Lewis acids when handling this compound. Overall, the ritterazine H eastern half is prepared in 14 steps and 6% yield from hecogenin acetate, or in 98% yield from the ritterazine B eastern half.

**Structural Analysis of the Synthetic Spiroketal Diastereomers.** The stereochemistry of all six 5,5-spiroketal prepared was verified by a pattern of nuclear Overhauser effects (NOEs) (Figure 1) and, in the case of the ritterazine G and F eastern halves, by X-ray crystallography (Figure 2).

For ritterazine G (**7**, Figure 1), both the NOEs and the X-ray crystal structure reveal a conformation stabilized by two anomeric effects, where the spiroketal carbon–oxygen bond lengths are 1.42 and 1.43 Å, consistent with values expected for anomeric carbon–oxygen bonds in 5,5-spiroketal.<sup>24</sup> In comparison, the diastereomer of ritterazine G (**8**) interconverts rapidly (on the NMR time scale) between conformations having one and two anomeric effects. The strongest NOEs are consistent with the extended conformation (Figure 1b), which possesses only one anomeric effect, but we also observed a weak NOE consistent with a bent structure that has two anomeric effects (see Figure 3); the number and intensities of the NOEs suggest that the extended conformation is preferred despite its diminished anomeric stabilization. Consequently, the diastereomer of ritterazine G may provide a particularly convenient model for studying anomeric effects in 5,5-spiroketal, which are less well understood than in 6,6-spiroketal.<sup>51,52</sup>

In comparison, the eastern halves of ritterazines B and H (**17** and **18**), in which the C22 spiroketal is in the *R* configuration,



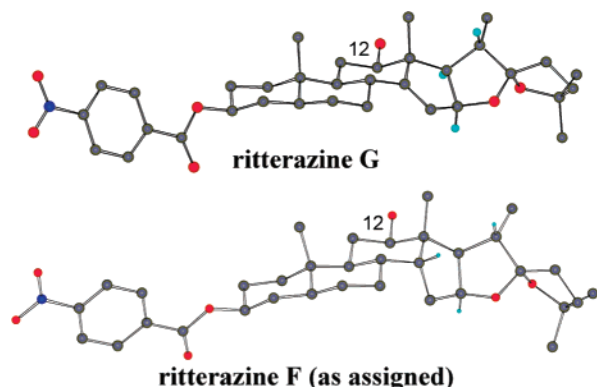
**Figure 1.** Representative NOEs for the ritterazine eastern halves. The NOEs are separated into their backbone and spiroketal components. The intensities of the NOEs are indicated by color: red, strong; black, medium; blue, weak.

show solution conformations favoring single anomeric effects; no NOEs were found that support a conformation with two anomeric effects. This result implies that the *cis*-hydrindane induces a greater steric bias toward an extended spiroketal conformation than does the olefin in the ritterazine G diastereomer (**8**).

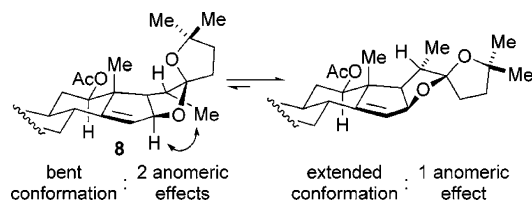
**Comparison of Synthetic Ritterazines B, F, G, and H with Their Natural Analogues.** Because the ritterazines are linear dimers of two steroidal units and because the two halves are separated by a large distance (the molecules are ~30 Å long),

(51) Perron, F.; Albizzati, K. F. *Chem. Rev.* **1989**, *89*, 1617–1661.

(52) Aho, J. E.; Pihko, P. M.; Rissa, T. K. *Chem. Rev.* **2005**, *105*, 4406–4440.



**Figure 2.** X-ray crystal structures for the ritterazine G and F eastern halves. The crystals are of the *p*-nitrobenzoyl derivatives of ritterazines G and F, which were prepared according to the procedures outlined in the Supporting Information. The *p*-nitrobenzoate group was removed from carbon 12 for clarity.



**Figure 3.** NOEs for the diastereomer of ritterazine G showing the conformational equilibrium in  $C_6D_6$  at 20 °C.

the presence or absence of one half should have little impact on the chemical shifts of protons near the ends of the other half (i.e., near the C22 spiroketal units). This hypothesis is supported by the nearly identical chemical shifts for the synthetic ritterazine G eastern half and for those of the natural product (Figure 4a).<sup>1,3</sup> In Figure 4a, select proton chemical shifts for natural ritterazine G are shown on the left, with deviations from these values for each synthetic spiroketal epimer shown to the right. Positive values for  $\Delta\delta$  correspond to chemical shifts that are further upfield from those for the natural product, whereas negative values are for protons further downfield. Comparison of the values in Figure 4a confirms that the spiroketal stereochemistry in synthetic diastereomer **9** is the same as that originally assigned. Similar correlations, however, were not found for ritterazines B and F (see b and c of Figure 4, respectively). For these systems, the chemical shifts for natural ritterazine B match diastereomer **13** (the thermodynamically favored spiroketal), not diastereomer **17** as assigned in the isolation paper.<sup>1</sup> Likewise, ritterazine F matches the spiroketal in the nonanomeric configuration (**17**), not the thermodynamically favored spiroketal as originally proposed. This reassignment does not conflict with the data obtained by the authors of the isolation papers; in their case, the spiroketals were assigned on the basis of a single and somewhat ambiguous NOE; other correlations were absent because of poor NOE buildup due to the unfavorable correlation times of the full-length natural product.<sup>1</sup> However, the reduced size of our synthetic halves has allowed a complete NOE analysis.

This reassignment is consistent with the distribution of the ritterazine natural products: the ritterazine B eastern half was originally assigned as the spiroketal in the nonanomeric configuration, but this spiroketal is conserved among seven natural products. Ritterazine F, on the other hand, was assigned as the thermodynamically favored spiroketal, but its spiroketal appears

in only one natural product. Our reassignment reverses the trend: now ritterazine B and six other ritterazine natural products have the thermodynamically favored spiroketal, whereas ritterazine F has the spiroketal in the nonanomeric configuration; this result is intellectually satisfying, particularly if the spiroketals equilibrate in ocean water. However, while such an equilibration seems reasonable, there are additional data that contradict this idea: ritterazine H possesses the nonanomeric spiroketal, but the corresponding thermodynamically favored spiroketal has not been isolated. This issue of whether ritterazines equilibrate in nature will be discussed in more detail below.

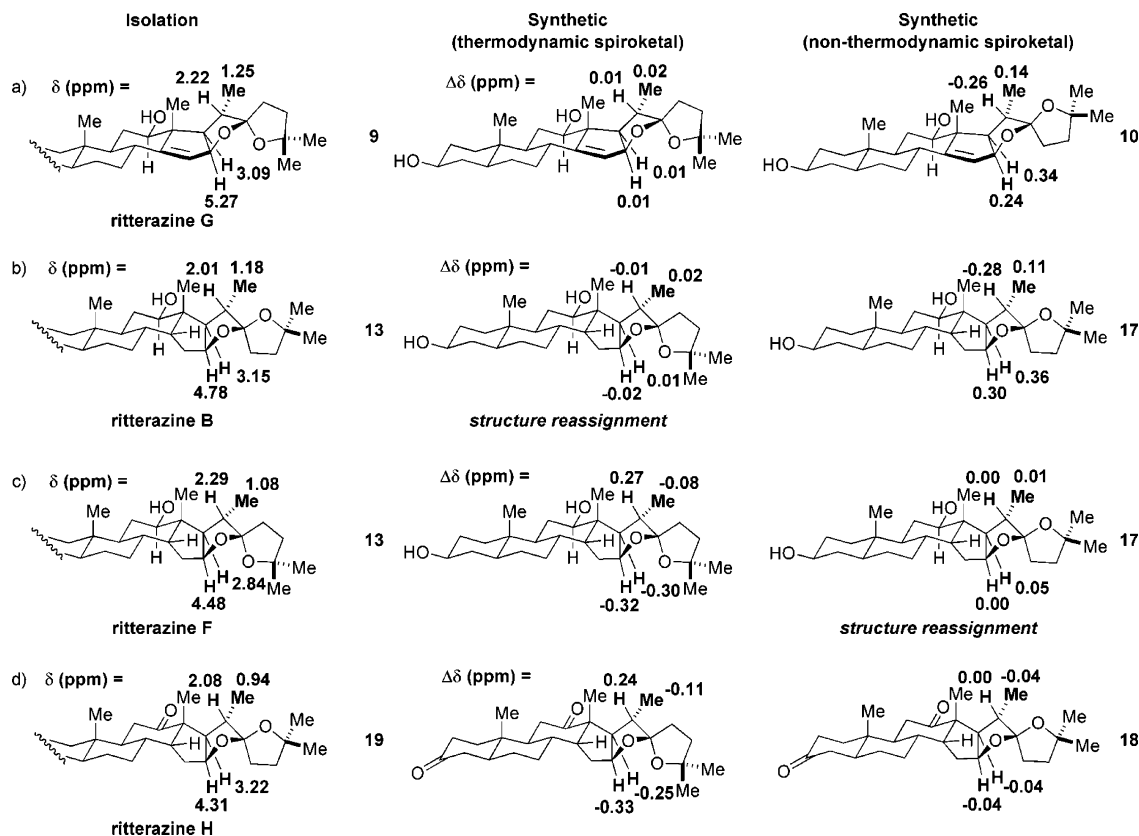
The reassignment of ritterazines B and F (and consequently ritterazines C, P, Q, R, S, and Y) is further supported by a trend of downfield chemical shifts for protons in proximity to the terminal spiroketal oxygen (Figure 5). For example, when the terminal oxygen of the C22 spiroketal is  $\alpha$ -configured (thermodynamically favored configuration), then the two steroid protons (H16 and H17) in close proximity are shifted ca. 0.2–0.3 ppm downfield relative to when the spiroketal oxygen is  $\beta$  (nonanomeric configuration). Similarly, the proton (H20) in proximity to the  $\beta$ -oxygen is shifted 0.2–0.3 ppm downfield as compared to the  $\alpha$ -diastereomer.

These downfield changes in chemical shifts are due to the deshielding effect of the nearby electronegative oxygen atom.<sup>53</sup> A similar phenomenon has been observed in 2-*endo*-norborneol, where the alcohol lone pairs interact through space with nearby protons and perturb their chemical shifts in an angle-dependent manner.<sup>53–55</sup> Not surprisingly, this effect is also distance-dependent. In our systems, a rough correlation exists between larger  $\Delta\delta$  values and smaller distances between the C16 proton and the terminal spiroketal oxygen (Figure 5):  $\Delta\delta = 0.23$  ppm for **9** versus **10**, with a hydrogen–oxygen distance of 2.94 Å,<sup>56</sup>  $\Delta\delta = 0.29$  ppm for **19** versus **18**, with a hydrogen–oxygen distance of 2.88 Å,<sup>57</sup> and  $\Delta\delta = 0.32$  ppm for **13** versus **17**, with a hydrogen–oxygen distance of 2.84 Å.<sup>58</sup>

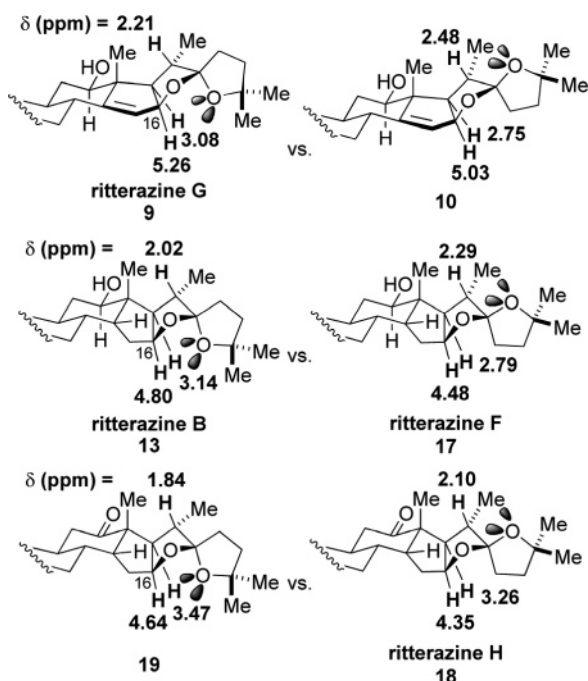
**Equilibration of Ritterazines in Ocean Water.** Since we had access to all spiroketal epimers of the eastern halves of ritterazines B, F, G, and H, we decided to investigate why there is an uneven distribution of the C22 spiroketal epimers in nature. This required that we determine whether the ritterazines equilibrate in ocean water, and if they did, then we needed to study the kinetics and mechanism(s) for this process so that we could understand the relationship between structure and rates of equilibration. The results of these studies are presented below.

We are uncertain about the exact environment within the tunicates (or possible symbiotic organisms) that produce the ritterazines (salinity, acidity, etc.),<sup>59</sup> but we reason that ocean water should reflect the conditions under which the ritterazines were found and should serve as an appropriate medium to

- (53) Seidl, P. R.; Carneiro, J. W. de M.; Tostes, J. G. R.; Koch, A.; Kleinpeter, E. *J. Phys. Chem. A* **2005**, *109*, 802–806.
- (54) Seidl, P. R.; Tostes, J. G. R.; Carneiro, J. W. de M.; Taft, C. A.; Dias, J. F. *J. Mol. Struct.* **2001**, *539*, 163–169.
- (55) Abraham, R. J.; Barlow, A. P.; Rowan, A. E. *Magn. Reson. Chem.* **1989**, *27*, 1074–1084.
- (56) Distances were obtained from the X-ray crystal structure of the eastern half of ritterazine G, shown in Figure 2.
- (57) Distances were calculated from the minimum energy conformation found from a Monte Carlo conformational search using the MM2\* force field.
- (58) Distances were obtained from the X-ray crystal structure of the ritterazine B eastern half, shown in Figure 2.
- (59) The ritterazines were isolated from the tunicate *R. tokioka* in waters with an average temperature of 21 °C: Fukuzawa, S. Personal communication.



**Figure 4.** Comparison of proton chemical shifts for ritterazines B, F, G, and H with those of their synthetic counterparts. Proton chemical shifts were measured at 22 °C in pyridine-*d*<sub>5</sub>. Values for the synthetic derivatives are shown as differences between the natural product chemical shift<sup>1,3</sup> and the synthetic chemical shift:  $\Delta\delta = \delta_{\text{natural}} - \delta_{\text{synthetic}}$ .



**Figure 5.** Effect of spiroketal stereochemistry on proton chemical shifts (pyridine-*d*<sub>5</sub>, 22 °C).

measure whether these spiroketals equilibrate naturally. Shown in Table 1 are data indicating the extent to which ritterazine

5,5-spiroketals equilibrate in ocean water. These results demonstrate that ocean water does catalyze the equilibration of the spiroketals, albeit at vastly different rates for each ritterazine spiroketal. For example, the C22 diastereomer of the eastern half of ritterazine G (**10**) equilibrates nearly 50% after 4 days at 40 °C, and after 33 days only 6% of the starting spiroketal epimer remains; this result explains why ritterazine G was isolated, but its C22 diastereomer was not. However, given the equilibrium ratio between ritterazine G and its diastereomer (line 3, Table 1), we would expect a small quantity of the diastereomer to exist in nature. Using the equilibrium ratio as a guide, we estimate that ca. 132  $\mu\text{g}$  of ritterazine G's diastereomer should have been present along with the 2.2 mg of ritterazine G found in the 8.2 kg of tunicates used in the isolation process.<sup>3</sup>

In contrast to the rapid equilibration of ritterazine G's epimer, only 4% of ritterazine F equilibrates after 4 days at 40 °C, and 50% conversion is not reached until 24 days.<sup>62</sup> The differences in equilibration rates are even more pronounced with ritterazine H, where only 1% epimerizes after 4 days at 40 °C. This slow conversion explains why this spiroketal with the nonanomeric configuration persists in nature.

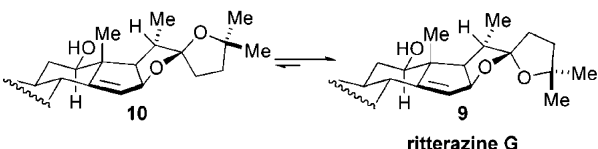

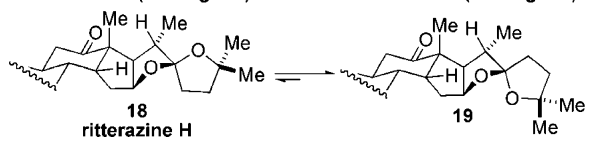
These results raise the question of what catalyzes the equilibration in ocean water; magnesium(II) clearly catalyzes the equilibration in organic solvent, but the catalytic species in ocean water is less obvious. Lines 4–6 in Table 1 outline our efforts to determine the identity of this catalyst. For example, the diastereomer of ritterazine G equilibrates slowly in carbonate-

(60) Pusztai, A. *Biochem. J.* **1966**, *99*, 93–101.

(61) Cohn, E. J.; Conant, J. B. *Proc. Natl. Acad. Sci. U.S.A.* **1926**, *12*, 433–438.

(62) The equilibration of ritterazine F may or may not be relevant to its native environment, depending on the lifetime of the ritterazines within the tunicate.

Table 1. Equilibration of the Nonanomeric Spiroketal in Ocean Water

Reaction	Solvent <sup>a,b</sup>	Additive	Temp. (°C)	Time (d)	Ratio of S.M. : Product <sup>c</sup>	$\Delta G^\circ$ (kcal/mol) <sup>d</sup>
 ritterazine G	ocean H <sub>2</sub> O pH = 8.21	none	23	15	74 : 26	—
	ocean H <sub>2</sub> O pH = 8.21	none	40	3.9	53 : 47	—
	ocean H <sub>2</sub> O pH = 8.21	none	40	33.2	6 : 94	1.6
	carbonate buffer pH = 8.10	none	40	3.9	91 : 9	—
	carbonate buffer pH = 8.10	MgCl <sub>2</sub> (53.1 mM)	40	3.9	16 : 84	—
	H <sub>2</sub> O pH = 7.08	none	40	3.9	4 : 96	1.9
 ritterazine B (reassigned)	ocean H <sub>2</sub> O pH = 8.21	none	40	3.9	96 : 4	—
	ocean H <sub>2</sub> O pH = 8.21	none	40	24	47 : 53	—
 ritterazine H	ocean H <sub>2</sub> O pH = 8.21	none	40	3.9	99 : 1	—

<sup>a</sup> Aqueous solvents were mixed with acetone in a 1:1 ratio to ensure solubility of the compounds. <sup>b</sup> Ocean water was collected from Crane Beach, Ipswich, MA, and organics were removed prior to use.<sup>60,61</sup> <sup>c</sup> Ratios were determined by <sup>1</sup>H NMR analysis. <sup>d</sup>  $\Delta G^\circ$  values were calculated at 298 K using the equation  $\Delta G^\circ = -RT \ln K$ .

buffered water, but the equilibration is faster when MgCl<sub>2</sub> is added to mimic the magnesium(II) dissolved in ocean water (on average, ocean water has 53.1 mM magnesium(II)<sup>63</sup>). However, the pH within the tunicate also may be relevant to the rate of spiroketal equilibration<sup>64</sup> because even 10-fold more acidic water equilibrates the diastereomer of ritterazine G more quickly (line 6, Table 1).

**Kinetics Studies on Ritterazine Equilibration.** The various rates of spiroketal equilibration in ocean water are consistent with the natural distribution of the ritterazine 5,5-spiroketal, but it is not clear why these structurally similar systems have such different behavior. To address this question, we performed a series of kinetics and mechanistic experiments on *p*-nitrobenzoylated derivatives of the ritterazine halves. These studies were performed in organic solvents, where the equilibration rates are faster and, therefore, more convenient to monitor relative to the rates in ocean water. Also, we measured the equilibration rates for each ritterazine half at six different temperatures, which allowed us to calculate and compare the free energy values for the transition states ( $\Delta G^\ddagger$ ) (Table 2).

The magnitudes of the transition-state free energies ( $\Delta G^\ddagger$ ) shown in Table 2 are low, which is consistent with the rapid equilibration of these spiroketals at room temperature, but it is the  $\Delta\Delta G^\ddagger$  values ( $\Delta G^\ddagger_{\text{ritH}} - \Delta G^\ddagger_{\text{ritB}}$  and  $\Delta G^\ddagger_{\text{ritH}} - \Delta G^\ddagger_{\text{ritG}}$ ) that highlight the differences in reaction rates between spiroketals. The relationship between reaction rate and  $\Delta G^\ddagger$  can be described quantitatively in terms of half-lives by modification of the Eyring equation, as follows:

$$k = \kappa \frac{k_B T}{h} e^{-\Delta G^\ddagger/RT} \Rightarrow T_{1/2} = \ln 2 \left( \kappa \frac{k_B T}{h} e^{-\Delta G^\ddagger/RT} \right)^{-1}$$

This equation reveals the exponential dependence of half-lives

on  $\Delta G^\ddagger$ , which explains why seemingly small values for  $\Delta\Delta G^\ddagger$  correspond to large differences in reaction rates. For example, the  $\Delta G^\ddagger$  value for the ritterazine H eastern half is only 1.8 kcal·mol<sup>-1</sup> higher than that for the diastereomer of ritterazine G, but the half-life for ritterazine H is nearly 35 times longer. The ritterazine F eastern half, on the other hand, equilibrates only 2-fold faster than ritterazine H, due to the mere 0.6 kcal·mol<sup>-1</sup> difference in transition-state free energies. Clearly, small structural differences between the ritterazine eastern halves have large ramifications on the equilibration rates by influencing the free energy of the transition states.

**Mechanistic Studies on Ritterazine Equilibration.** Ritterazines F and H and the diastereomer of ritterazine G are structurally very similar, but as shown in the kinetics studies above, the free energies of the transition states are different, which leads to their unique rates of equilibration. To eliminate the possibility that the differences in transition-state free energies are the result of differences in mechanism, we performed two experiments to determine which oxonium ion is operative in the transition state.

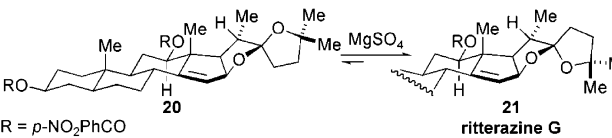
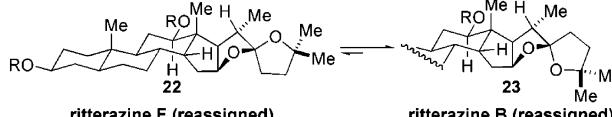
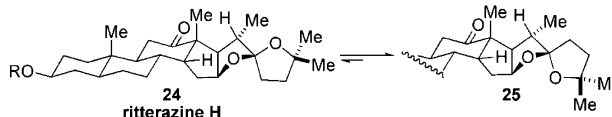
The first experiment involved trapping the oxonium ion with a hydride source (Scheme 5); we assumed that both possible oxonium ion intermediates would reduce at equal rates and that the rate of reduction would not be limiting, both of which are plausible in cases where a large excess of the reductant is used. A single reduction product was observed for each reaction shown in Scheme 5, indicating that the three compounds equilibrate by the same mechanism, which involves opening of the terminal spiroketal ring. In each example, the identity of the product was determined using a combination of <sup>1</sup>H chemical

(63) Akhtar, W.; Zaidi, I. A. S. S. H.; Jilani, S. *Water, Air, Soil Pollut.* **1997**, *94*, 99–107.

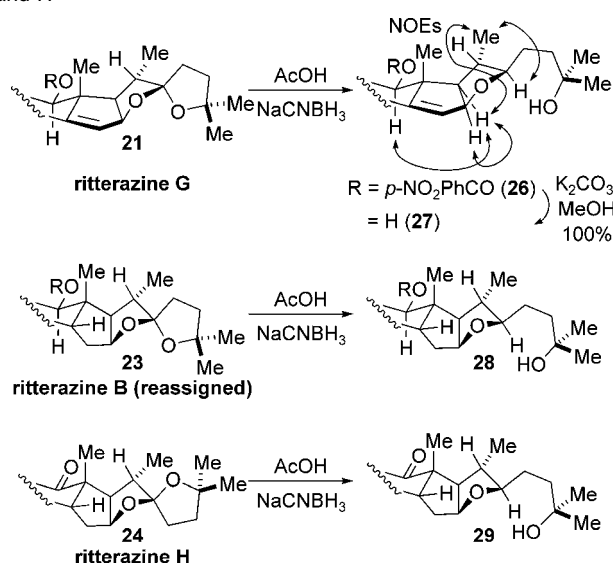
(64) Doney, S. C. *Sci. Am.* **2006**, *294*, 58–65.



**Table 2.** Equilibration of the Ritterazine F, G, and H Nonanomeric Spiroketal in Toluene<sup>a</sup>

Reaction <sup>b</sup>	T <sub>1/2</sub> @ 25 °C (s)	ΔG° (kcal/mol) <sup>c</sup>	ΔG <sup>‡</sup> (kcal/mol) <sup>d</sup>	ΔΔG <sup>‡</sup> (kcal/mol)	ΔH <sup>‡</sup> (kcal/mol) <sup>e</sup>	ΔS <sup>‡</sup> (cal/mol) <sup>e</sup>
 ritterazine G	6	-1.6±0.1	19.1±0.1	1.8	17.6±0.5	-4±2
 ritterazine F (reassigned)      ritterazine B (reassigned)	99	-1.8±0.1	20.3±0.2	0.6	20.4±0.7	0±3
 ritterazine H	209	-1.8±0.1	20.9±0.1	0	23±1	6±5

<sup>a</sup> Reactions were run at six temperatures using a 500 μM concentration of the compound in toluene and 1000 equiv of MgSO<sub>4</sub>. Equilibrations were performed in triplicate, taking eight time points per temperature; diastereomer ratios were determined by integration of HPLC peak areas. Temperatures were chosen to cover a 40-fold change in reaction rate for each spiroketal. <sup>b</sup> The preparation of these labeled derivatives is outlined in the Supporting Information. <sup>c</sup> ΔG° values were calculated at 298 K from the equation ΔG° = -RT ln K<sub>eq</sub>, where values for K<sub>eq</sub> were measured 3–8 times at 23 °C. <sup>d</sup> ΔG<sup>‡</sup> values are reported at 298 K and were calculated from the following equation: ΔG<sup>‡</sup> = ΔH<sup>‡</sup> - TΔS<sup>‡</sup>. <sup>e</sup> ΔH<sup>‡</sup> and ΔS<sup>‡</sup> values were calculated from a plot of ln(kT<sup>-1</sup>) versus T<sup>-1</sup> and are reported as the average of three independent measurements.

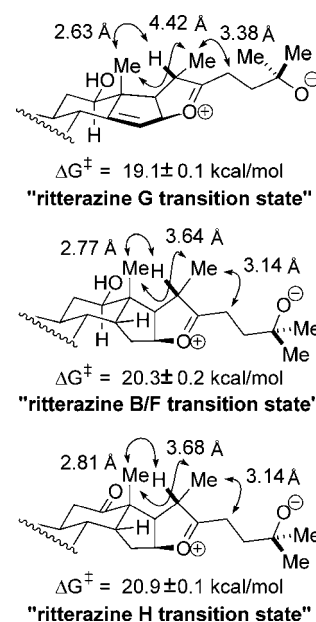
**Scheme 5.** Mechanism of Equilibration for Ritterazines B, G, and H<sup>a</sup>

<sup>a</sup> The reduction reactions were quantitative, as determined by integration of the <sup>1</sup>H NMR spectrum.

shift and NOE data, where representative NOEs are shown only for the diastereomer of ritterazine G. The structure of this product was further confirmed by comparison of its deprotected derivative (27) with the acetate-deprotected version of intermediate 6 that was prepared by an independent route (Scheme 1).

The second experiment involved the measurement of entropy contributions to the transition-state free energies. In this case, the mechanism suggested by the trapping experiments is supported by the nearly equivalent ΔS<sup>‡</sup> values for all three compounds (Table 2). The other possible transition state would have two additional rotatable bonds, which would increase the ΔS<sup>‡</sup> term by ca. 14 cal·mol<sup>-1</sup>, a value that would be distinguishable among the ΔS<sup>‡</sup> values shown in Table 2.<sup>65</sup> Our experimental

(65) Searle, M. S.; Williams, D. H. *J. Am. Chem. Soc.* **1992**, *114*, 10690–10697.



**Figure 6.** Transition-state models from molecular mechanics simulations. The low-energy transition states were calculated from Monte Carlo searches using the MMFF force field<sup>68</sup> provided in the Spartan modeling package. Calculated atom distances are included as a measure of unfavorable nonbonding interactions: methyl–methyl distances are measured between carbons, while methyl–hydrogen distances are measured between the methyl carbon and the hydrogen of interest.

values, however, are all approximately zero, which is consistent with a common mechanism and is frequently observed in cases where solvent becomes more ordered around the charged transition states.<sup>66,67</sup>

Since ritterazines B, G, and H equilibrate through the same mechanism, the different ΔG<sup>‡</sup> values, and consequently the different equilibration rates, must arise from minor structural

(66) Carpenter, B. K. *Determination of Organic Reaction Mechanisms*; John Wiley & Sons: New York, 1984.

(67) Zuman, P.; Patel, R. C. *Techniques in Organic Reaction Kinetics*; John Wiley & Sons: New York, 1984.

variations in the transition state. Monte Carlo conformational searches for all three transition states<sup>68</sup> reveal increasing A(1,2) strain and *syn*-pentane interactions moving from ritterazine G to B to H, which accounts for the higher  $\Delta G^\ddagger$  values found in the latter (Figure 6). These unfavorable nonbonding interactions are both distant- and angle-dependent; the distances are shown in Figure 6 to highlight the increasing strain between the transition states. Ultimately, the natural distribution of the ritterazine 5,5-spiroketal is more a function of the transition-state free energies ( $\Delta G^\ddagger$ ) than of the ground-state free energies ( $\Delta G^\circ$ ), and even small deviations in the steroid backbone affect the energy of the transition states and, therefore, the rate of spiroketal equilibration.

### Conclusion

We have developed short, efficient, and scalable routes to the eastern halves of ritterazines B, F, G, and H and to the spiroketal epimers of ritterazines G and H, and in doing so, we have reassigned the spiroketal stereochemistry for the eastern halves of ritterazines B and F. Our syntheses also demonstrate a convenient strategy for preparing spiroketal-substituted *cis*-hydrindanes. Consequently, we now have a route that could produce large quantities of 10 ritterazine eastern halves, which is an important step toward our ultimate goal of uncovering

the cellular target of these molecules and of determining which elements of their structures are important for biological activity. Finally, equilibration of these ritterazine 5,5-spiroketal in toluene and in ocean water has led to the observation that minor and remote structural features on the steroid backbone can impact the free energy of the transition states for spiroketal equilibration; in fact, the transition-state free energies dictate the natural distribution of the ritterazine spiroketals much more than the ground-state free energies.

**Acknowledgment.** This work was supported by Novartis Institutes of Biomedical Research. S.T.P. is a Damon Runyon Fellow supported by the Damon Runyon Cancer Research Foundation (Grant DRG-1805-04). We also thank Neil Vasani and Amy L. Wojciechowski for their contributions at the outset of the program. The crystal structures for compounds **21** and **23** were solved by Dr. Richard J. Staples of the X-ray Crystallographic Laboratory at Harvard University.

**Supporting Information Available:** Experimental procedures and characterization for the compounds described above, tabulation of kinetics data, and CIF files for compounds **21** and **23**. This material is available free of charge via the Internet at <http://pubs.acs.org>.

JA0705487

(68) Gundertofte, K.; Liljefors, T.; Norrby, P.; Pettersson, I. *J. Comput. Chem.* **1996**, *17*, 429–449.